GAS TRANSFER ACROSS GAS-LIQUID BOUNDARIES: PREDICTIONS AND EXPERIMENTS ON CONCENTRATION FLUCTUATIONS

Johannes Gérson Janzen
Escola de Engenharia de São Carlos – Universidade de São Paulo
jgersonj@gmx.net

Gerhard Jirka
Institut für Hydromechanik – Universität Karlsruhe
jirka@uka.de

Harry Edmar Schulz
Escola de Engenharia de São Carlos – Universidade de São Paulo
heschulz@sc.usp.br

Abstract. *Experiments have been conducted to understand the basic principles involved in the interfacial gas transfer mechanism under liquid-side control. Planar concentration fields of the dissolved oxygen near the air-water interface have been quantificated in an oscillating-grid tank using a laser induced fluorescence (LIF) technique. The high data resolution is an advantage for revealing the concentration distribution within the concentration boundary layer, which is only a few hundred of micrometers thick. Vertical profiles from the mean concentration and fluctuation intensity were obtained from the concentration fields. The fluctuation intensity profiles were compared with a theoretical analysis.*

Keywords*: laser induced fluorescence, oscillating-grid tank, air-water gas transfer*

1. Introduction

Gas transfer across air-water interface is an important process for many environmental and industrial systems. To understand the basic principles involved in this phenomenon, a detailed understanding of the interfacial region is desirable, where the mass transfer process is controlled by thin boundary layers. The details of these boundary layers are determined by the aero and hydrodynamics near the air-water interface. For slightly soluble gases, such as oxygen, the gas transfer is controlled predominantly by the aqueous mass boundary layer (Lewis and Whitman, 1924). This layer is about ten to hundred μm thick, which implies that measurements near the interface are very difficult to be conducted. Recently, laser induced fluorescence (LIF) techniques have been employed in studies of gas transfer across air-water interfaces. Such techniques allow to obtain a detailed knowledge of the concentration fields near the interface and so to improve predictive models.

In this study, a LIF technique is employed to investigate the oxygen transfer process across an air-water interface in an oscillating-grid tank. The data measured with this technique permit to obtain mean concentration and *rms* concentration profiles. The *rms* concentration profiles are compared with Schulz and Schulz's (1991) theoretical analysis.

2. Theoretical Background

The mass transfer of a compound across the air-water interface is typically described by

$$\frac{dC_B}{dt} = K\left(C_S - C_B\right) \tag{1}$$

where K is the gas transfer coefficient (s^{-1}), C_S the saturation concentration (kg/m^3), C_B the bulk concentration (kg/m^3), and t the time (s). It follows that

$$\frac{C_B - C_S}{C_0 - C_S} = \exp\left(-Kt\right) \tag{2}$$

where C_0 is the concentration at $t = 0$. Equation (2) shows that the time evolution of the normalized gas concentration does not depend of any spatial coordinate. However, there is a strong variation in the time averaged gas concentration in the region immediately below the surface. Therefore, Lee and Luck (1982), Schulz and Schulz (1991), and Chu and

Jirka (1992), suggested a normalized form to describe the behavior of the mean concentration along the direction normal to the surface, *z*, as

$$\frac{C(z)-C_B}{C_S-C_B}=f(z)=C^*(z) \tag{3}$$

where *C(z)* is the mean gas concentration at a point in the water. Equations (2) and (3) represent the form of analyses performed for the time and spatial evolutions of the mean gas concentration in liquids that is found in the literature.

2.1 Analysis of concentration fluctuation

Assuming no effect of diffusivity over the concentration fluctuations near the surface, the simplified record of concentration suggested by Schulz and Schulz (1991), in a form of a random square wave, may be used and is reproduced in Fig. 1.

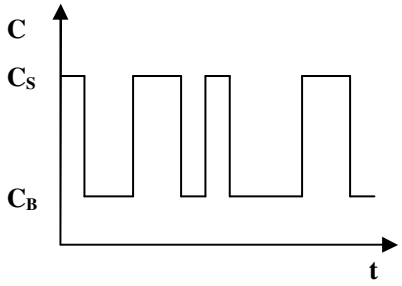

Figure 1. Random square wave for concentration evolution in time

The concentration time evolution for a point located in the superficial layer is assumed as an alternance between saturation concentration C_S and bulk concentration C_B. Defining *n* as

$$n=\frac{t_S}{t_M} \tag{4}$$

$$1-n=\frac{t_B}{t_M} \tag{5}$$

where t_S is the time with $C = C_S$, t_B is the time with $C = C_B$, and t_M is the measurement time. *n* and *(n-1)* are function of *z*. The mean value of the concentration *C*, is given by

$$C=nC_S+(1-n)C_B \tag{6}$$

The values of the fluctuations, above and under the mean value, are

$$c_1=(1-n)(C_S-C_B) \tag{7}$$

$$c_2=n(C_S-C_B) \tag{8}$$

The mean square of the fluctuations is defined as

$$c'^2=\overline{(C_{ins}-C)^2} \tag{9}$$

where C_{ins} is the instantaneous concentration at a point in the liquid. The bar indicates a time average operation. Using Eqs. (4) to (9) we have:

$$c'^2 = (C_S - C_B)^2 (1-n) n \tag{10}$$

The concentration fluctuation intensity defined as the square root of Eq. (9), and normalized with ($C_S - C_B$), is

$$\frac{c'}{(C_S - C_B)} = \sqrt{(1-n)n} \tag{11}$$

It is necessary, now, to evaluate n as function of z. Subtracting C_B from Eq. (6) leads to

$$\frac{C - C_B}{C_S - C_B} = n \tag{12}$$

From Eqs. (3) and (12) we have:

$$n = f(z) \tag{13}$$

From Eqs. (11) and (13) we have:

$$\frac{c'}{(C_S - C_B)} = \sqrt{[1 - f(z)] f(z)} \tag{14}$$

3. Experimental Methods

3.1. Oscillating Grid System

Oscillating grids have been commonly used to generate controlled turbulent fields in viscous fluids, thereby allowing a better understanding of the turbulence effect on several physical phenomena. A grid (usually square) with mesh size M oscillates around a mean position with amplitude S (the stroke) at a frequency f in a tank filled with a viscous fluid. The turbulence in the bulk of the tank is the result of the interaction between jets and wakes produced by the movement of the grid. The mean velocity of the flow is zero and turbulence decays with increasing distance from the grid. Literature shows that beyond a distance ranging from one to three mesh sizes from the grid, turbulence is homogeneous on planes parallel to the grid, with a ratio of vertical to horizontal turbulent intensities in the range of 1.1-1.3.

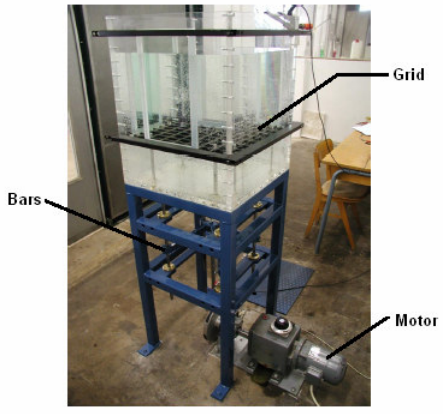

Figure 2. View of the experimental apparatus.

Figure 2 is a view of the oscillating-grid tank used in this study. The experiments were conducted in a tank made of Perspex, with a 0.50 m x 0.50 m square cross-section and 0.65 m height. A grid with 6.35 cm mesh size was built, which resulted in a solidity of 36%. This grid design fulfills the condition proposed by Hopfinger and Toly (1976), who

stated that stable jets and wakes could be obtained only with a solidity of less than 40 %. The grid was positioned 20.0 cm above the bottom of the tank to avoid secondary motions. The grid was operated with a 5.0 cm stroke S and the frequency f was varied from 2.0 to 5.0 Hz. The water depth h was around 28.0 cm (water surface to grid). The water temperature was 26.5 ^{o}C. Table 1 presents experimental parameters, where Re is the Reynolds number defined as fS^2/ν. Because the oscillating grid turbulence is sensitive to the initial conditions, data acquisition could only begin 10 min after the onset of oscillation (Cheng and Law, 2001).

Table 1. Experimental Parameters

Run no.	f (Hz)	S (cm)	Re	z_0 (mm)
1	2	5	5785	0.324
2	3	5	8677	0.269
3	4	5	11570	0.261
4	5	5	14452	0.230

3.2. Laser Induced Fluorescence (LIF) technique

A Laser Induced Fluorescence (LIF) technique is employed to obtain dissolved oxygen concentration fields at the air-water interface. Vaughan and Weber (1970) demonstrated that pyrene butyric acid (PBA) can be used as an adequate indicator for dissolved oxygen concentration in water, considering its fluorescence lifetime and intensity change in the presence of oxygen. The change in fluorescence lifetime τ and intensity F, also called quenching, is quantitatively described by the Stern-Volmer equation:

$$\frac{F_0}{F} = \frac{\tau_0}{\tau} = 1 + K_{SV} C \tag{15}$$

where F_0 and τ_0 are the fluorescence intensity and lifetime, respectively, in the absence of the quencher and K_{SV} is the Stern-Volmer quenching constant. Hence, the quencher concentration (in this case dissolved oxygen) can be determined by measuring the intensity of emitted fluorescence (in this case PBA). Münsterer, Mayer and Jähne (1995) and Herlina and Jirka (2004) found a K_{SV} value of 683±70 l/mol.

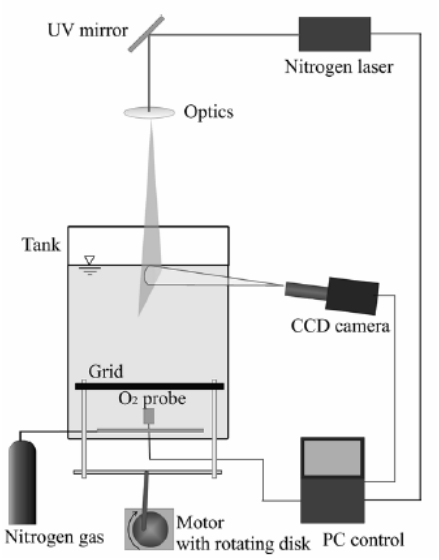

Figure 3. Experimental set-up and LIF configuration (Herlina and Jirka, 2004)

Figure 3 shows the LIF setup used in this study. The tank was filled with $2x10^{-5}$ M PBA. Water in the tank was bubbled with nitrogen to remove oxygen. An initially dissolved oxygen concentration of about 0.7 mg/l was achieved after 20 minutes of bubbling. A pulsed nitrogen laser (MNL 801) with a mean energy power of 0.4 mJ and a wavelength emission of 337.1 nm was used to excite the PBA solution. The laser beam was guided into the centre of the tank through a UV-mirror and a combination of lenses. A FlowMaster CCD camera (1024 x 1280 pixels and 12 bit), with a macro objective was used to obtain images of approximately 9.5 mm x 11.9 mm from a distance of about 30 cm.

Therefore, the measurements have a resolution of approximately 9 μm. The PBA fluorescence intensity lies between 370-410 nm. An optical bandpass filter was mounted in front of the camera in order to ensure that only the fluorescent light could pass trough. Restricted by the RAM capacity of the computer, the maximum number of successive images is limited to 300. 900 images were taken for each run.

3.2.1 Image Processing

A raw image is shown in Fig. 4. A series of image-correction steps must be performed on the raw images before the concentration information can be extracted. These steps include noise removal, water surface location, correction of laser attenuation, and correction of optical blurring near the interface.

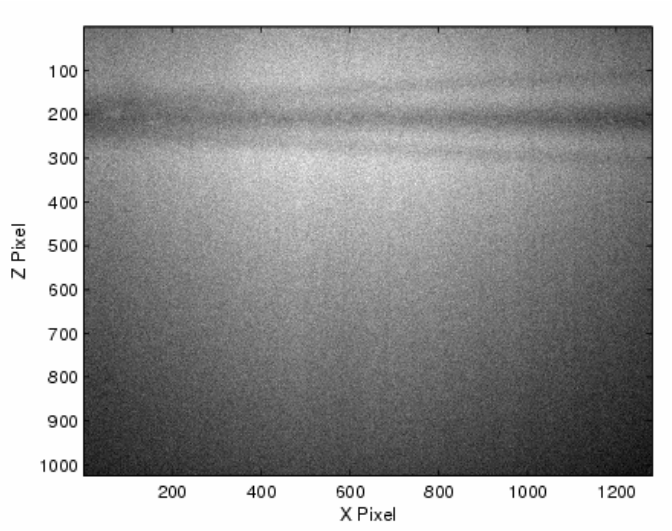

Figure 4. Raw fluorescence image.

Firstly, 10 iterations of filtering in the horizontal direction x and 5 iterations in the vertical direction z were carried out to remove noise. An adaptive filter with filter size of 9 pixels was applied in the z direction. In the x direction, the filter size was 19 pixels. The different filtering size was chosen because the changes along the horizontal direction are not so abrupt as in the vertical direction. Figure 5 shows an example of a vertical intensity profile before and after the noise removal.

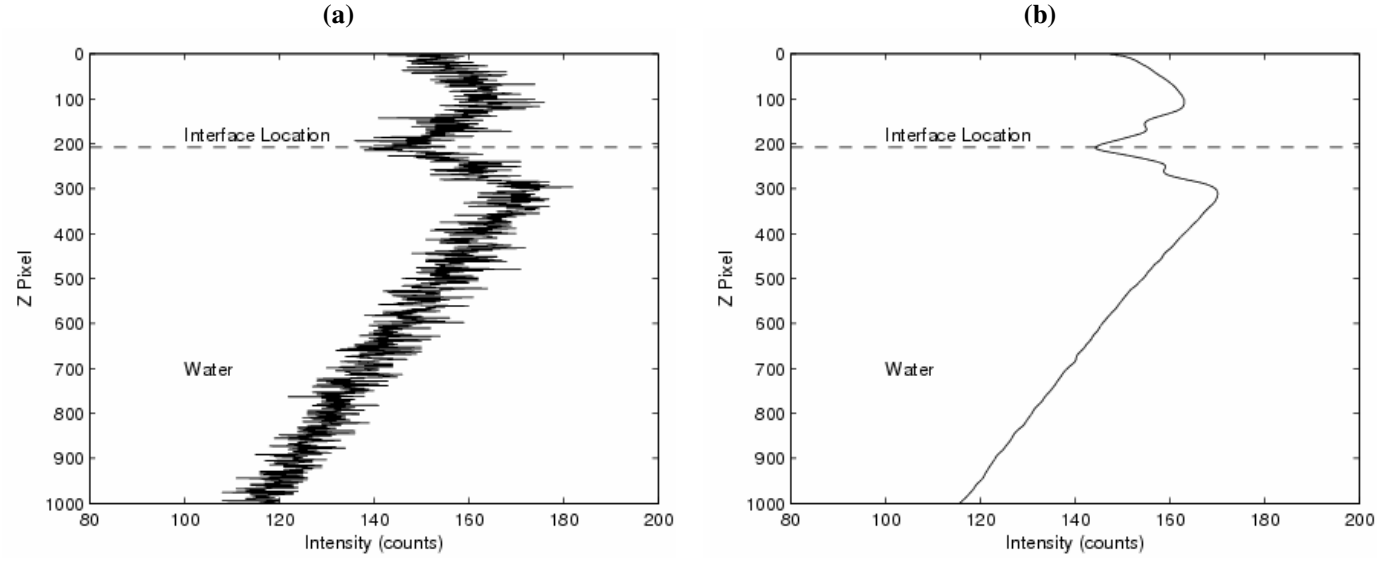

Figure 5. Column intensity profile from Fig. 4: (a) prior and (b) after adaptive filtering.

It can also be observed, in Fig. 5, that there is a reflection at the water surface. The location of the interface could thus be detected by searching for the reflective symmetry line. Evaluating a single vertical column, the symmetry point

would be at the zero-crossing of the first derivative of the profile. The Canny method was used to detect the zero-crossing.

As the light sheet travels trough the water (containing PBA), there is an exponential decrease of the fluorescence intensity. This effect, usually denominated Lambert-Beer decay, is described by the equation

$$\frac{I}{I_0} = \exp\left(-\alpha \cdot C_{PBA} \cdot l\right) \tag{16}$$

where I is the energy of the laser in the fluid at the position l, I_0 is the energy of the laser as it enters the fluids, α is a constant, C_{PBA} is the concentration of the fluorescent molecule, and l is the distance traveled trough the fluid. The Lambert-Beers decay for each column is determined by fitting an exponential curve in the bulk region. Figure 6a shows the exponential Lambert-Beer decays for the filtered vertical column in Fig. 5. The Lambert-Beer effect on each vertical column was then corrected by dividing the recorded intensity by the exponent of Lambert-Beers equation.

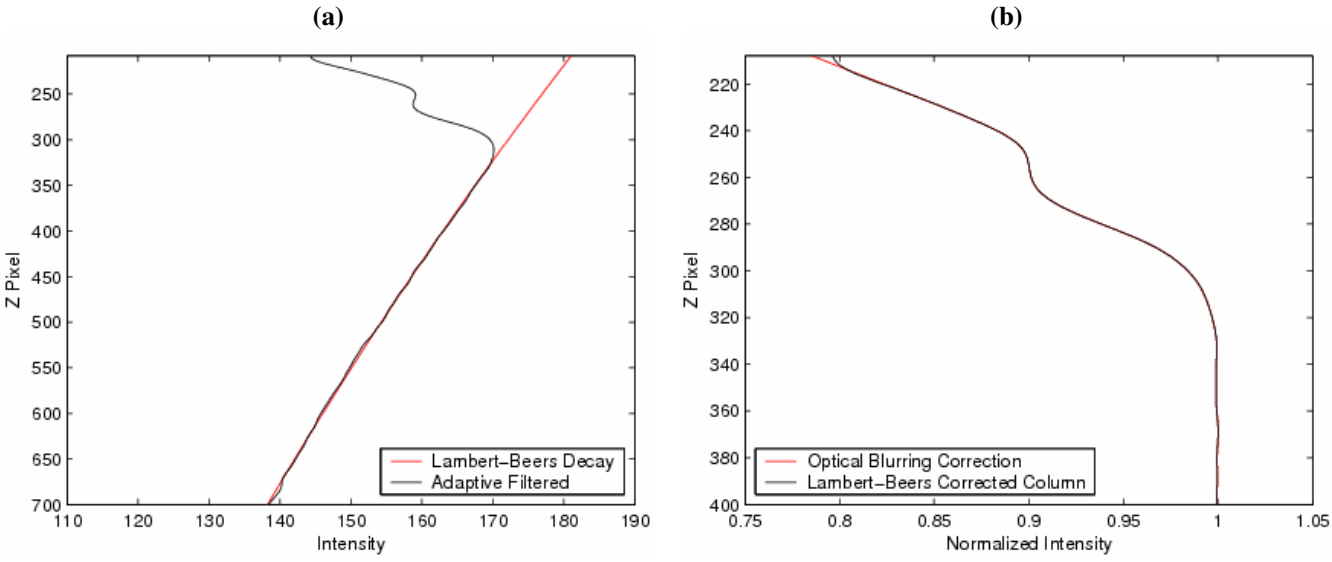

Figure 6. (a) Curve fit for Lambert-Beers decay from Fig. 5; (b) Normalized intensity and optical blurring correction from Fig. 6a.

The Lambert-Beers-corrected column profiles present a diminishing of the gradients near the interface, rather than the expected sharp and increasing gradients (as shown in Fig. 6b). The same phenomenon has been noted in similar experiments (Woodrow and Duke, 2001; Herlina and Jirka, 2004). The blurring effect is corrected by extrapolating the sharpest gradient up to the interface.

Finally, the concentration information can be extracted. The dissolved oxygen concentration can be expressed in a dimensionless form

$$C^*(z) = \frac{C(z) - C_B}{C_S - C_B} = \frac{F_I\left[F_B - F(z)\right]}{F(z)\left[F_B - F_I\right]} \tag{17}$$

where F_i and F_B are, respectively, the fluorescence intensity at the interface and in the bulk liquid. Therefore, the value of the dimensionless concentration varies from 1.0 at the interface to 0.0 in the bulk. Figure 7 presents the vertical normalized concentration profile from Fig. 6.

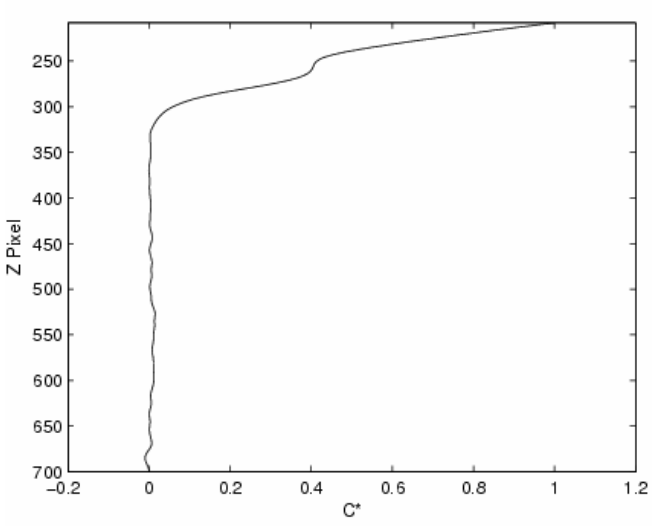

Figure 7. Vertical concentration profile from Fig. 6.

4. Results and Discussion

4.1 Mean Concentration

Figure 8a presents the mean concentration profiles for different runs. The profiles for high turbulence conditions have a steeper (sharper) gradient than those for low turbulence conditions. Chu and Jirka (1991) suggested an exponential approximation for describe the behavior of the mean concentration along z, as

$$\frac{C(z)-C_B}{C_S-C_B} = f(z) = \exp\left(-\frac{z}{z_0}\right) \tag{18}$$

where z_0 (with dimension of length) can be interpreted as a concentration boundary layer thickness. Table 1 presents the values of z_0. It can be observed that z_0 decreases for greater turbulent conditions.

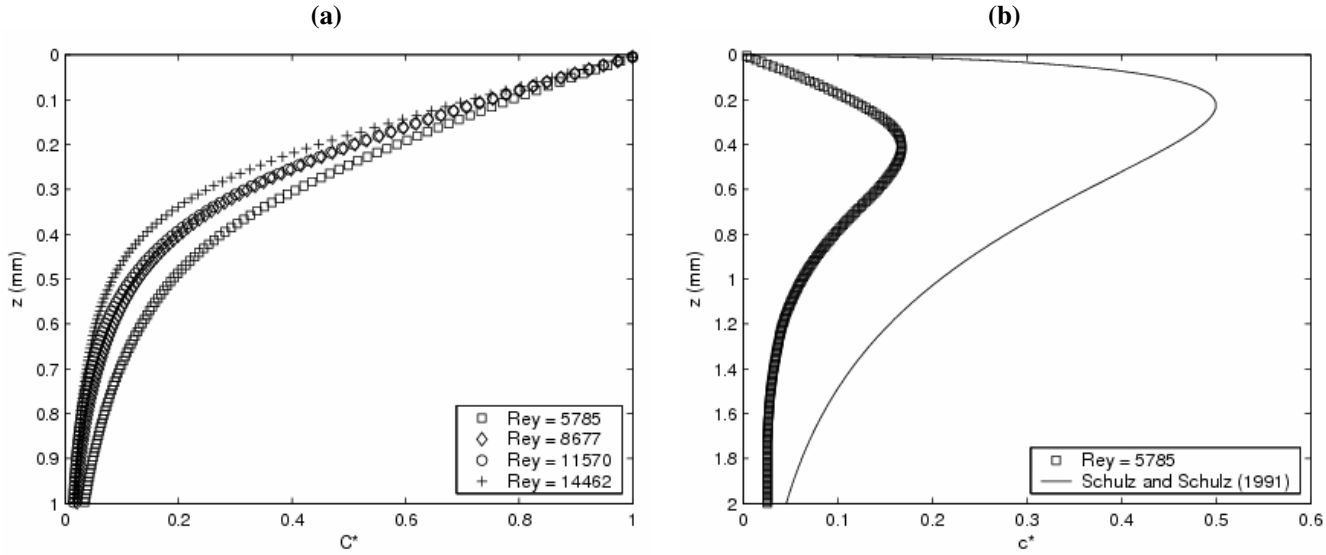

Figure 8. (a) Mean concentration profiles; (b) *RMS* concentration profiles.

4.2 *RMS* Concentration

Figure 8b presents the *rms* concentration *c*' normalized by the difference of concentration between the interface and the bulk $(C_S - C_B)$ for run 1. Substituting Eq. (18) into Eq. (14), we obtain

$$c^* = \frac{c'}{(C_S - C_B)} = \sqrt{\left[1 - \exp\left(-\frac{z}{z_0}\right)\right]\exp\left(-\frac{z}{z_0}\right)} \tag{19}$$

As previously stated, Eq. (14) represents the extreme case in which the molecular diffusivity does not contribute for the establishment of the *rms* concentration profiles. Although this situation not represents the actual phenomena, it allows to infer that a maximum peak occurs below the surface and that this maximum is always less than 0.5, i.e.,

$$c^*_{PEAK} = \left[\frac{c'}{(C_S - C_B)}\right]_{PEAK} < 0.5 . \tag{20}$$

The present peak values are in the range of about 0.13 to 0.17. These results support the conclusion of Eq. (20).

5. Conclusions

The interaction between gas transfer and bottom shear induced turbulence was studied experimentally in an oscillating-grid tank using a LIF technique. Vertical mean and *rms* concentration profiles were obtained from the concentration fields. The mean concentration profile showed steeper gradient for high turbulent conditions than those for low turbulent conditions. It could also be observed that a maximum peak of the fluctuation intensity profile occurs below the surface. A simplified theoretical analysis permits conclude that the value of the maximum peak must be lower than 0.5.

6. Acknowledgements

The authors are indebted to the Brazilian Council of Research and Technology (CNPq) and to the São Paulo Research Support Foundation (FAPESP).

7. References

Cheng, N.S. and Law, A.W.K., 2001, "Measurements of Turbulence Generated by Oscillating Grid", Journal of Hydraulic Engineering, Vol. 127, No. 3, pp. 201-208.

Chu, C.R. and Jirka, G.H., 1992, "Turbulent Gas Flux Measurements Below the Air-Water Interface of a Grid-Stirred Tank", Int. J. Heat Mass Transfer, Vol. 35, No. 8, pp. 1957-1968.

Herlina and Jirka, G.H., 2004, "Application of LIF to Investigate Gas Transfer Near the Air-Water Interface in a Grid-Stirred Tank", Experiments in Fluids, Vol. 37, pp. 341-349.

Hopfinger, E.J. and Toly, J.-A., 1976, "Spatially Decaying Turbulence and its Relation to Mixing Across Density Interfaces", J. Fluid Mech., Vol. 78, pp. 155-175.

Lee, Y.H. and Luk, S., 1982, "Characterization of Concentration Boundary Layer in Oxygen Absorption", Ind. Eng. Chem. Fundam., Vol. 21, No. 4, pp. 428-434.

Lewis, W.K. and Whitman, W.G., 1924, "Principles of Gas Absorption", Industrial and Engineering Chemistry, Vol. 16, No. 12, pp. 1215-1220.

Schulz, H.E. and Schulz, S.A.G., 1991, "Modelling Below-Surface Characteristics in Water Reaeration", Water Pollution: Modelling, Measuring and Prediction, Southampton, England, pp. 441-454.

Münsterer, T., Mayer, H. and Jähne, B., 1995, "Dual-Tracer Measurements of Concentration Profiles in the Aqueous Mass Boundary Layer", Air-Water Gas Transfer: 3rd Int. Symp. on Air-Water Gas Transfer, pp. 637-648.

8. Responsibility notice

The authors are the only responsible for the printed material included in this paper.